

# Supplementary Material

for

## Identification of Si-vacancy related room temperature qubits in 4H silicon carbide

Viktor Ivády,<sup>1,2,\*</sup> Joel Davidsson,<sup>1</sup> Nguyen Tien Son,<sup>1</sup>  
Takeshi Ohshima,<sup>3</sup> Igor A. Abrikosov,<sup>1,4</sup> and Adam Gali<sup>2,5,†</sup>

<sup>1</sup>*Department of Physics, Chemistry and Biology,  
Linköping University, SE-581 83 Linköping, Sweden*

<sup>2</sup>*Wigner Research Centre for Physics, Hungarian Academy of Sciences,  
PO Box 49, H-1525, Budapest, Hungary*

<sup>3</sup>*National Institutes for Quantum and Radiological Science and Technology,  
1233 Watanuki, Takasaki, Gunma 370-1292, Japan*

<sup>4</sup>*Materials Modeling and Development Laboratory,  
National University of Science and Technology 'MISIS', 119049 Moscow, Russia*

<sup>5</sup>*Department of Atomic Physics, Budapest University of Technology and Economics,  
Budafoki út 8., H-1111 Budapest, Hungary*

(Dated: October 13, 2017)

## HYPERFINE STRUCTURE OF NEGATIVE SILICON VACANCY - NEUTRAL CARBON VACANCY PAIR

As can be seen in the main text, the  $V_{\text{Si}}(-) + V_{\text{C}}(0)$  defect has spin-1/2 ground state. The quartets excited state is 1.3 eV higher in energy than the doublet ground state. In Table SI, we provide hyperfine coupling parameters for  $V_{\text{Si}}(-) + V_{\text{C}}(0)$  defect. Due to the spin-1/2 ground state, the calculated hyperfine structure does not resemble the hyperfine structure of V2 center.

TABLE SI. Hyperfine parameters of the silicon vacancy-carbon vacancy model for V2 center in 4H-SiC.

site	distance from $V_{\text{Si}}$ (Å)	multiplicity	$A_{xx}$ (MHz)	$A_{yy}$ (MHz)	$A_{zz}$ (MHz)
$C_{V\text{Si}1a}$	2.089	1	80.966	80.966	265.973
$C_{V\text{Si}1b}$	2.096	3	7.467	7.309	16.164
$\text{Si}_{V\text{Si}1a}$	3.084	3	28.233	27.691	31.102
$\text{Si}_{V\text{Si}1b}$	3.075	6	1.796	0.967	1.831
$\text{Si}_{V\text{Si}1b} = \text{Si}_{V\text{C}1b}$	3.137	3	4.042	3.083	6.507

## EPR MEASUREMENTS

The PL lines V1-V3 in 4H SiC and 6H SiC are known to be related to the electron paramagnetic resonance (EPR) centers  $T_{V1a}$ - $T_{V3a}$  in these polytypes. Our EPR measurements were performed on a Bruker X-band EPR spectrometer. In order to increase the concentration of the Si vacancy, we use high-purity semi-insulating (HPSI) 4H and 6H-SiC bulk samples with large size of (typically 2 mm  $\times$  3 mm  $\times$  20 mm) irradiated by 2 MeV electrons at room temperature with fluences in the range of 2 - 8  $\times 10^{18}$  cm $^{-2}$  to create very high concentrations of the Si vacancy. After irradiation, the samples were annealed at  $\sim 400$  °C to eliminate interstitial-related defects, whose signals usually cover the whole range of studied magnetic field, causing serious overlapping with the spectrum of the Si vacancies.

Fig. 3 in the main text shows the EPR spectrum of the  $T_{V1a}$  and  $T_{V2a}$  in 4H SiC measured at 292 K for the magnetic field  $B$  parallel to the  $c$ -axis ( $B \parallel c$ ). The  $T_{V1a}$  signals can be resolved from the hyperfine (hf) structure due to the interaction between the electron spin and the nuclear spin of one  $^{29}\text{Si}$  nucleus ( $I = 1/2$ , 4.68% natural abundance) occupying one of 12 second neighbor

Si sites. The splitting of 3.66 G for  $T_{V1a}$  corresponds to a zero-field splitting of 0.915 G (or  $\sim 2.56$  MHz) for a spin  $3/2$  center. This value is in agreement with the value reported by Janzén *et al.* (Ref. 26 in the main text). At the  $c$ -direction, the hf splitting of 12 second neighbor Si is found to be  $\sim 8.4$  MHz for  $T_{V2a}$  and  $\sim 8.2$  MHz for  $T_{V1a}$ . As can be seen in the inset of Fig. 3 of the main text, a small hf splitting of  $\sim 0.8$  MHz is observed. Judging from the intensity, these hf lines should be related to the hf interaction with  $^{29}\text{Si}$  nuclei in further neighbor shells beyond the second neighbor.

The hf structures due to interaction between the electron spin and the nuclear spin of one  $^{13}\text{C}$  nucleus ( $I = 1/2$ , 1.07% natural abundance) occupying one of four nearest neighbor C sites for  $T_{V1a}$  and  $T_{V2a}$  in  $4H$  SiC at the direction of the  $c$ -axis are shown in Fig. S1. At this direction, the interactions with three C in the basal plane are equivalent, giving rise to the same pair of resonance lines with three times of intensity as compared to that of the hf interaction with the C along the  $c$ -axis. A slightly larger hf splitting of 3 C is observed for  $T_{V1a}$  compared to that of  $T_{V2a}$ . The zero-field and hf splittings for these centers in  $4H$  SiC are given in Table I of the main text.

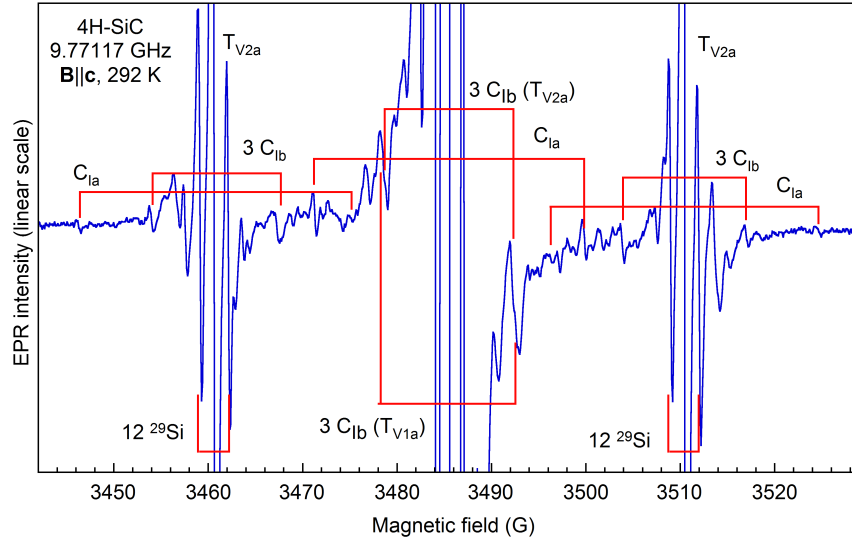


FIG. S1. EPR spectrum in  $4H$  SiC irradiated to a fluence of  $8 \times 10^{18} \text{ cm}^{-2}$  measured in darkness at 292 K for  $B \parallel c$  showing the C hf structures due to the interaction with the C atom along the  $c$ -axis (labeled as 1 C) and with three C atoms in the basal plane (labeled as 3 C) for  $T_{V1a}$  and  $T_{V2a}$ . The MW power is 2.012 mW and the field modulation is 0.2 G. The 3 C hf structure of central line of  $T_{V1a}$  and  $T_{V2a}$  can be resolved when using a field modulation of 0.1 G (not shown).

The EPR signals of the  $T_{V1a}$ ,  $T_{V2a}$  and  $T_{V3a}$  centers in  $6H$  SiC measured in darkness at 293 K

for  $B \parallel c$  are shown in Fig. S2. The zero-field splittings of these centers are in agreement with the reported data in Ref. 26 in the main text. The 1 C and 3 C hf structures of  $T_{V1a}$ ,  $T_{V2a}$  and  $T_{V3a}$  centers at the  $c$ -direction are shown in Fig. S3.

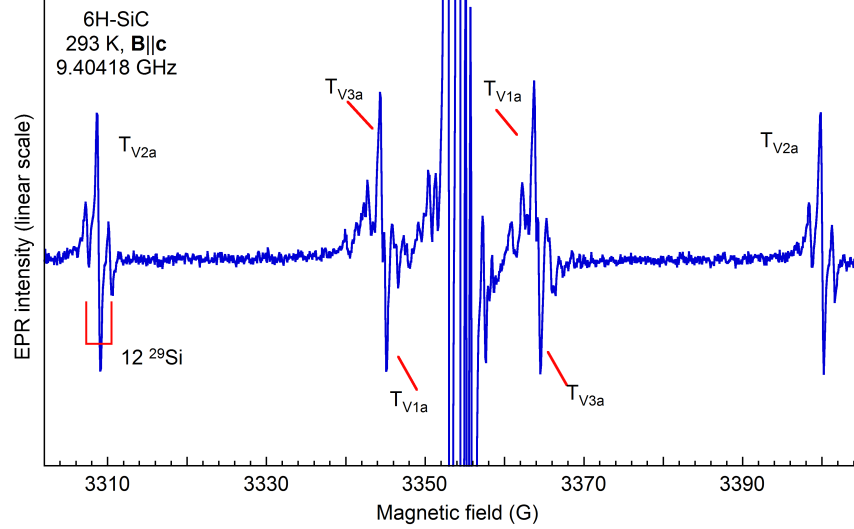


FIG. S2. EPR spectrum in 6H SiC irradiated to a fluence of  $2 \times 10^{18} \text{ cm}^{-2}$  measured in darkness at 293 K for  $B \parallel c$  showing the zero-field splitting of the  $T_{V1a}$ ,  $T_{V2a}$  and  $T_{V3a}$  centers. The MW power is  $6.325 \mu\text{W}$  and the field modulation is 0.3 G.

### THEORETICAL HYPERFINE PARAMETERS FOR $V_{\text{Si}}^-$ IN 4H SiC

In Table SII and Table SIII we provide the hyperfine parameters of the strongest coupled nuclei for an isolated negatively charged silicon vacancy defect at the  $h$  and  $k$  configurations, respectively. For  $^{29}\text{Si}$  both negative and positive hyperfine parameters are found indicating the sign change of the spin density at farther neighbor shells.

### THEORETICAL RESULTS FOR $V_{\text{Si}}^-$ IN 6H SiC

In Table SIV, one can see calculated and measured magneto-optical data for V1-V3 centers in 6H-SiC. Similarly to the case of 4H-SiC, non-zero ZFS is obtained for all the different silicon vacancy configurations. The calculated properties of the isolated silicon vacancies are in good agreement with the experimental parameters. The V1, V2, and V3 centers in 6H-SiC may tentatively be associated with  $h$ ,  $k_1$  and  $k_2$  configurations, respectively, based on the order of ZFS

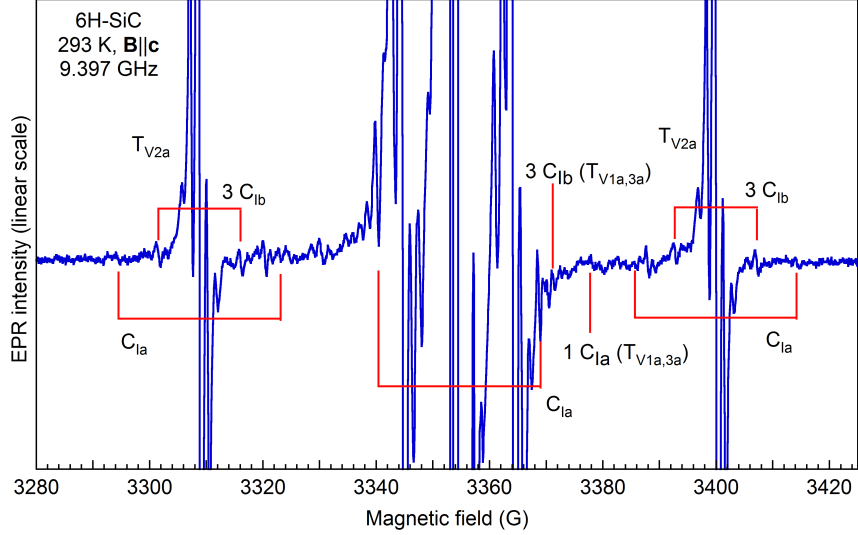


FIG. S3. EPR spectrum in 6H SiC irradiated to a fluence of  $8 \times 10^{18} \text{ cm}^{-2}$  measured in darkness at 293 K for  $B \parallel c$  showing the hyperfine structures of 1 and 3 nearest C neighbors of  $T_{V1a}$ ,  $T_{V2a}$  and  $T_{V3a}$  centers. Although the main lines of  $T_{V1a}$  and  $T_{V3a}$  are resolved, their hf lines could not be distinguished. The spectrum was measured with the same parameters as given in Fig.S2.

constants. ZFS is related to the ground state property and very sensitive to the geometry of the carbon dangling bonds that should be well calculated by DFT. By using this argument, the quasi cubic  $V_{Si}(-)$  would give rise the room temperature qubits in 6H-SiC. Further studies are needed for unambiguous identification in the less experimentally explored and studied 6H-SiC.

In Table SV, we list  $^{29}\text{Si}$  sites around an isolated silicon vacancy in 6H SiC for which negative hyperfine splittings are obtained in our first-principles calculations.

---

\* vikiv@ifm.liu.se

† gali.adam@wigner.mta.hu

TABLE SII. Table of calculated hyperfine eigenvalues for  $^{29}\text{Si}$  and  $^{13}\text{C}$  nuclei adjacent to a negatively charged silicon vacancy at the  $h$  configuration (associated with V1 center) in  $4H$  SiC. Theoretical values are listed for those nuclei sites where the absolute average of the hyperfine tensor eigenvalues are larger than 0.65 MHz. Distances from the vacancy and multiplicity of the sites are also provided.

site	distance from $V_{\text{Si}}$ ( $\text{\AA}$ )	multiplicity	$A_{xx}$ (MHz)	$A_{yy}$ (MHz)	$A_{zz}$ (MHz)
C <sub>Ia</sub>	2.033	1	32.7	32.7	85.5
C <sub>Ib</sub>	2.029	3	31.5	31.4	85.1
Si <sub>IIa</sub>	3.055	3	8.194	8.470	7.384
Si <sub>IIb</sub>	3.057	6	7.553	7.906	6.959
Si <sub>IIc</sub>	3.058	3	7.684	8.029	7.277
C <sub>Va</sub>	4.740	3	3.725	3.665	7.131
C <sub>Vb</sub>	4.741	6	3.986	3.932	7.470
C <sub>Vc</sub>	4.745	3	3.879	3.805	7.132
Si <sub>VIIIa</sub>	6.150	3	-1.239	-1.153	-2.098
Si <sub>VIIIb</sub>	6.144	6	-1.142	-1.130	-2.086
Si <sub>VIIIc</sub>	6.150	3	-1.430	-1.419	-2.364
C <sub>XIIIa</sub>	7.775	3	0.500	0.481	0.951
C <sub>XIIIb</sub>	7.758	6	0.474	0.464	0.948

TABLE SIII. Table of calculated hyperfine eigenvalues for  $^{29}\text{Si}$  and  $^{13}\text{C}$  nuclei adjacent to a negatively charged silicon vacancy at the  $k$  configuration (associated with V2 center) in  $4H$  SiC. Theoretical values are listed for those nuclei sites where the absolute average of the hyperfine tensor eigenvalues are larger than 0.65 MHz. Distances from the vacancy and multiplicity of the sites are also provided.

site	distance from $V_{\text{Si}}$ ( $\text{\AA}$ )	multiplicity	$A_{xx}$ (MHz)	$A_{yy}$ (MHz)	$A_{zz}$ (MHz)
C <sub>Ia</sub>	2.034	1	34.096	34.096	84.746
C <sub>Ib</sub>	2.039	3	28.618	28.445	82.202
Si <sub>IIc</sub>	3.062	3	7.280	7.623	6.807
Si <sub>IIb</sub>	3.060	6	8.235	8.546	7.843
Si <sub>IIc</sub>	3.062	3	8.271	7.185	8.591
C <sub>III</sub>	3.139	1	1.835	1.835	0.483
C <sub>IV</sub>	3.609	3	0.838	0.949	0.179
Si <sub>V</sub>	4.341	3	0.739	0.807	0.387
C <sub>VI</sub>	4.398	6	1.049	1.011	2.514
C <sub>VIIa</sub>	4.757	3	4.300	4.182	7.690
C <sub>VIIb</sub>	4.741	6	4.628	4.595	8.191
Si <sub>VIIIa</sub>	5.007	1	-4.636	-4.636	-5.125
Si <sub>VIIIb</sub>	5.020	1	1.374	1.374	1.226
Si <sub>XIII</sub>	6.145	6	-1.632	-1.615	-2.823

TABLE SIV. Theoretical and experimental magneto-optical data for V1, V2, and V3 centers in 6H SiC. The hyperfine splitting at  $B \parallel c$  was determined for the first neighbor  $^{13}\text{C}$  nuclei on ( $1 \times C_{\text{Ia}}$ ) and out ( $3 \times C_{\text{Ib}}$ ) of the symmetry axis of the isolated silicon vacancy and the averaged hyperfine splitting for the twelve second neighbor  $^{29}\text{Si}$  sites ( $12 \times \tilde{\text{Si}}_{\text{II}}$ ). Experimental ZPL energies were reported in Ref. ? while the ZFS and the resolvable hyperfine values are determined by our ESR measurements. The good agreement between theory and experiment supporting the isolated silicon vacancy model of V1-V3 centers.

Center/ Configuration	ZFS (MHz)	ZPL (eV)	Hypefine splitting (MHz)		
			$1 \times C_{\text{Ia}}$	$3 \times C_{\text{Ib}}$	$12 \times \tilde{\text{Si}}_{\text{IIa}}$
Experiment					
V1	13.3	1.433	79.6	39.8	8.1
V2	64.0	1.398	79.9	40.4	8.2
V3	13.9	1.368	78.6	39.8	8.2
Theory					
$V_{\text{Si}}^- @ h$	3.8	1.560	85.5	40.4	7.7
$V_{\text{Si}}^- @ k_2$	97.4	1.493	85.4	38.6	7.9
$V_{\text{Si}}^- @ k_1$	26.8	1.499	85.1	41.8	7.5



TABLE SV. List of  $^{29}\text{Si}$  sites close to an isolated negatively charged silicon vacancy in  $6H$  SiC for which negative hyperfine splitting is obtained.

site	distance from $V_{\text{Si}}$ ( $\text{\AA}$ )	multiplicity	$A_{xx}$ (MHz)	$A_{yy}$ (MHz)	$A_{zz}$ (MHz)
$V_{\text{Si}} @ h$					
Si <sub>VIIIa</sub>	6.145	3	-1.534	-1.523	-2.491
Si <sub>VIIIb</sub>	6.144	6	-1.160	-1.149	-2.105
Si <sub>VIIIc</sub>	6.146	3	-1.136	-1.127	-2.047
$V_{\text{Si}} @ k_1$					
Si <sub>XIIIa</sub>	6.144	6	-1.663	-1.647	-2.837
Si <sub>XIIIb</sub>	6.150	3	-1.300	-1.282	-2.238
$V_{\text{Si}} @ k_2$					
Si <sub>VIIIa</sub>	5.001	1	-4.451	-4.451	-4.933
Si <sub>XIIIb</sub>	6.144	6	-1.154	-1.142	-2.113
Si <sub>XIIIc</sub>	6.148	3	-1.376	-1.289	-2.290